Laser Scattering Measurements for Gas Densities in a Swirling Flow Combustor

R. N. Halthore* and F. C. Gouldin†
Cornell University, Ithaca, New York

Data in the form of mean and rms gas density profiles, mean methane density profiles, and selected gas density probability density functions and power spectral densities obtained by laser-induced Rayleigh and Raman scattering measurements in the primary zone of a premixed, swirling flow combustor are presented and discussed. Results are obtained with good repeatability (~6% for Raman and 4% for Rayleigh time-averaged measurements) and with good accuracy (~3%). Along with previously obtained velocity data, the data from scattering measurements are used to determine the region of chemical reaction relative to regions of flow recirculation and shear. Comparisons with previously obtained probe data for temperature and methane concentration indicate that probes may be unreliable for measurements in swirling flows.

Nomenclature

A = Avogadro number, 1/kg·mole
D = diameter of outer jet, 10.16 cm
f = frequency, Hz
G = autocorrelation function for photon fluctuations
i = index representing ith value in a set
K = constant
k = Boltzman constant, J/K
ℓ = length of the scattering volume
N = number of photons
N_b = number of photons due to background
N_0 = incident laser photon flux rate
$\{N(i,\Delta t)\}$ = set of instantaneous values of photon counts for counting period Δt
n = number density, 1/m^3
$\overline{n'^2}$ = variance in the number density
P = static pressure, assumed constant, N/m^2
P_0 = power of laser beam, arbitrary units
P_s = power of scattered light, units same as for P_0
R = radius of outer jet, 5.08 cm
R_i = radius of inner jet, 2.54 cm
$R(\tau_r)$ = autocorrelation function of number density for lag = τ_r
r = radial distance, cm
S_i = inner swirl number,
$$= \int_0^{R_i} \rho\tilde{u}\tilde{v}2\pi r^2 dr/R_i\left(\int_0^{R_i} \rho\tilde{u}^2 2\pi r dr\right)$$
S_0 = outer swirl number,
$$= \int_{R_i}^{R} \rho\tilde{u}\tilde{v}2\pi r^2 dr/R\left(\int_{R_i}^{R} \rho\tilde{u}^2 2\pi r dr\right)$$
$S(f)$ = power spectral density function
$T, \bar{T}$ = temperature and its time mean, K
u = axial velocity, m/s
$\tilde{u}$ = Favre averaged axial velocity
U_i = volume averaged inner jet velocity
U_o = volume averaged outer jet velocity
v = tangential velocity, m/s
W = molecular weight, kg/kg·mole
X = axial distance, cm
X_α = mole fraction of species α
α = species designation
Δt = counting period, time units
ϕ_i = inner flow equivalence ratio
ψ_r = stream function at r, equal to 1 at $X/D=0$, $r=R_i$
η = quantum efficiency of photomultiplier tube cathode
Ω = solid angle of collection
σ = cross section for Rayleigh or Raman scattering
τ = transmission efficiency of collection optics
τ_r = lag number

Presented as Paper 84-0199 at the AIAA 22nd Aerospace Sciences Meeting, Reno, NV, Jan. 9-12, 1984; received Dec. 22, 1984; revision received Sept. 10, 1985.

*Graduate Research Assistant in Mechanical and Aerospace Engineering, Sibley School of Mechanical and Aerospace Engineering (presently with Earth and Space Sciences, State University of New York, Stony Brook).

†Professor, Mechanical and Aerospace Engineering, Sibley School of Mechanical and Aerospace Engineering. Associate Fellow AIAA.

Introduction

THE importance of swirling flow effects on combustion in industrial burners, cyclone combustion chambers, and gas turbine combustors is well recognized. An extensive literature on the subject exists and several reviews are available.[1,2] Because the phenomena observed in swirling flow combustion are quite complex, there is general agreement that more research on the subject is required.

The combustor used for this study (Fig. 1) is composed of two concentric, confined swirling jets with an inner flow of air premixed with methane ($\phi_i = 0.8$) and an outer flow of air. The inner flow has a fixed swirl level, while swirl in the outer flow can be varied. The inner swirl is generated by admitting air to the inner flow tube through tangential slots machined in the tube wall well upstream of the test section, while the outer swirl is generated by adjustable vanes. The swirl levels are adjusted for these measurements such that a recirculation zone is precipitated on the combustor axis close to the inlet of the test section. In this work, two flow conditions are studied—one with swirl in the two jets in the same direction (coswirl) and one with swirl in opposite directions (counterswirl).

The motivation for conducting this research is threefold: 1) to provide an improved understanding of combustion processes in swirling flow with recirculation; 2) to perform measurements of time resolved density and time-averaged methane concentration using scattering methods so that a set of data complementary to existing velocity data is obtained to help in model evaluation and that a verification of suspected

probe perturbations can be made; and 3) to help extend the applicability of laser scattering techniques to more practical combustor environments than heretofore studied.

The research work on combustors using swirling flow is extensive. In much of this research, probes are used to measure time-averaged values of velocity and scalar fields. However, probe-induced flow perturbations are frequently observed in swirling flows[3-5] and there is concern regarding the validity of probe measurements in these flows. The increasing use of nonperturbing measurement techniques, such as laser Doppler velocimetry (LDV), is in part the result of such concern.

Not all swirling flow combustors have the same physical and chemical processes determining their performance. Some have premixed reactants (as is the case in the present study), while others involve liquid fuel injection. Also, different types of recirculation zones are observed. Thus, the results of the present work are comparable to a subset of all swirling flow combustion studies—those that have premixed reactants and a free-standing, closed, central recirculation zone—a subset that is quite small.

In the work of Beltagui and MacCallum,[6] a central recirculation zone is established at high degrees of swirl generated by hubless swirlers. The combustor used a premixed town-gas air flame. Mean temperature is found to peak at the edge, but just inside the recirculation zone. At a certain fuel/air ratio, oscillations are reported, but no details are given. They use thermocouples to measure the temperature and a water-cooled three-hole pressure probe to measure the velocity and static pressure. For CO_2 analysis, a sampling probe is used. Possible probe perturbations are not discussed.

Hubbed swirl generators are used by both Rhode et al.[7] and Brum and Samuelsen[8] and, thus, their flows are inherently different than ours. For example, Brum and Samuelsen[8] (who report LDV measurements) do not observe a free-standing recirculation zone but rather one attached to the swirler hub. Rhode et al.[7] use probes to measure the velocity in nonreacting flow and report the presence of a precessing vortex core downstream of the recirculation zone. As is the case for Beltagui and MacCallum, no probe-induced flow perturbations are reported.[7]

A series of studies have been conducted at Cornell in the swirling flow combustor used for the present study, as well as in a swirling flow apparatus of similar geometry.[9] In the latter study, measurements of mean velocity, rms velocity fluctuations, and static pressure were made using a five-holed pressure probe and a hot-wire anemometer. Besides delineating the recirculation zone, these measurements indicated the presence of periodic flow oscillations. Probe-induced flow distortion was not observed and comparison of these results with the laser velocimetry data obtained in an almost identical apparatus[10] supports this observation.

Research on the Cornell combustor includes the determination of blowoff limits.[11] Probe measurements for temperature and species concentration have been conducted in the primary zone[5,12] and at the exhaust of the combustor.[13,14] During these measurements, two types of perturbation were observed near the test section inlet: 1) the introduction of a cylindrical sampling probe very near the inlet precipitated a flame in the wake of the probe and 2) further downstream (at places where no visible probe perturbation is observed, but still near the inlet) appreciable mean methane concentration levels were measured in regions of high mean temperature.

LDV measurements in both isothermal and reaching flows[15] have been made that provide a picture of the mean flow patterns and turbulence levels in co- and counterswirling flow conditions. Chemiluminescent flame emission measurements[16] have helped to determine the location of the reaction zone in the combustor. Both the LDV and flame emission experiments suggest the presence of periodic oscillations of the flow and the reaction zone, respectively.

As a logical next step to these previous measurements, nonperturbing laser scattering measurements to determine total number density and CH_4 concentration were undertaken and the results are presented here.

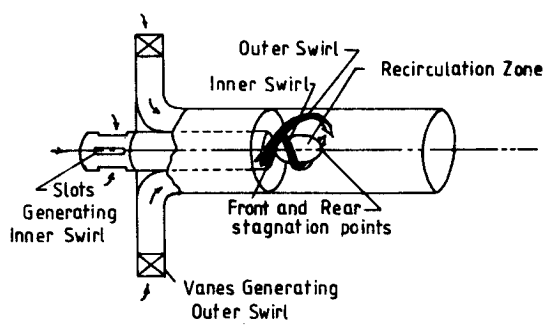

Fig. 1 Schematic of combustion apparatus showing swirl generating components and the test section. Fuel is injected into the inner flow from a tube lying along the centerline at a point just downstream of the swirl generator.

Experiment

Measurement Technique

The application of laser scattering techniques to measurements in reacting flows has been discussed in a number of articles and books (see, for example, Refs. 17-19). For both Rayleigh and Raman scattering, the power of scattered light from a laser beam is proportional to the number density of scattering molecules and, in general, is also a function of temperature. Thus, in principle, it is possible to measure by laser scattering both molecular number density and temperature.

In the case of Rayleigh scattering, it is difficult to resolve the line shape in real time and, in this case, the measured total scattered power is proportional to the total number density of molecules,

$$P_s = P_o \ell\, \Omega \eta \tau \Sigma \sigma_\alpha X_\alpha n = P_o K n \tag{1}$$

P_s depends on several factors, including the scattering efficiency of each chemical species as expressed by σ_α and its mole fraction. In general, both $\Sigma\sigma_\alpha X_\alpha$ and n are unknown variables and a Rayleigh measurement gives only their product. However, for a lean ($\phi = 0.8$) methane air mixture, the effective cross section $\sigma = \Sigma\sigma_\alpha X_\alpha$ of the mixture changes by less than 2% in going from reactants to stable products (CO_2 and H_2O). Because of the presence of CO in an equilibrium composition of products at high temperature, the effective cross section of hot products is slightly less than 96% of that of reactants, while higher levels of CO in the reaction zone reduce σ to approximately 94% of the reactant value.[20] Thus, in the central core of the combustor, where the dilution by mixing with the outer air flow is negligible, σ to good approximation is constant (within $\pm 3\%$) and a measure of P_s gives n. σ for air is 89% of that for a lean ($\phi = 0.8$) methane air mixture and, for measurements in regions where dilution is present, a maximum error of $\pm 5.5\%$ in n results when an average value for σ is used to interpret the data.

Raman scattering is an inelastic process and the scattered light forms a spectrum, the character of which depends on the scattering gas composition and temperature. The intensity of scattering associated with a single vibration/rotational transition can be estimated using Eq. (1). In principle, it is feasible to resolve this spectrum and to determine by experiment both the gas composition and the temperature. However, Raman scattering is a very weak process (two to three orders of magnitude weaker than Rayleigh) and, because of the low signal-to-noise levels, only time-averaged measurements are possible in the present experiment. Furthermore, since the scattered power is a nonlinear function of temperature and species concentration, the results of such time-averaged

measurements are difficult to interpret in terms of concentration and temperature.[18] If the scattered power in an entire band (or branch of a band) is measured, the temperature dependency is reduced greatly, since contributions from all of the rotational states are observed and because the vibrational excitation is small for the temperatures of interest (e.g., for methane, $\nu_1 = 2916.5$ cm^{-1}). Thus, a broad band measurement can give concentration data with little uncertainty. However, for a band or branch that is spectrally broad, the detection band is necessarily broad and background radiation (e.g., from the flame) can become a significant problem.

The methane molecule is a spherical top and the ν_1 fundamental is the most Raman active vibration. To very good approximation, this oscillation is harmonic. Thus, the Stokes Q-branches of hot bands are coincident with the cold Stokes Q-branch and it is possible to detect scattering from the entire branch structure with a narrow spectral window. (For the 5145 Å Ar^+ laser line, the Q-branch falls at 6053 Å.) Furthermore, the vibrational Raman scattering cross section for CH_4 is an order of magnitude higher than that for O_2 and N_2, making it feasible to measure relatively low levels of CH_4.

Apparatus

Figure 2 shows a schematic of the optical system. The scattering source is an A^+ laser operating at 5145 Å with an output power of 0.5-0.8 W. The laser beam, which is polarized vertically, is reflected off mirror M_1 to enter the combustor through slots cut in the test section wall. Lens L_1 focuses the beam onto a horizontal plane passing through the combustor axis. The beam exits the test section through another set of slots, either to a laser dump for Rayleigh scattering or to a mirror that reflects the beam back through the scattering volume in a multipassing configuration for Raman scattering. The reflection is slightly off axis to avoid coupling with the laser cavity. Multipassing increases the effective laser power in the scattering volume from 0.8 W (single pass) to 3.2 W.

Scattered light is collected at right angles to both the laser beam and the combustor axis and collimated by lens L_2. The collimated beam then passes through lens L_3 to be focused onto the entrance slit S of a monochromator. To achieve proper polarization for the scattered light and thereby maximize grating efficiency, a half-wave plate H is located between M_1 and the laser head, while the polarizer P in the collection optics reduces detected, unpolarized background light.

The dimensions of the cylindrical scattering volume as determined by the laser beam and collection optics are approximately 1 mm in height and 0.1 mm in diameter for Rayleigh scattering, while for Raman scattering, because of multipassing, the volume is approximated by a rectangular parallelepiped with a height of 1 mm, a width equal to 0.12 mm, and a depth equal to 0.18 mm. Light refraction at the combustor wall causes a small defocusing of the collection optics. However, since measurements are restricted to the central portion of the test section, this effect is small. The spatial resolution of the measurements is not materially affected and any changes in the photon collection efficiency of the detection optics are accounted for by calibration.

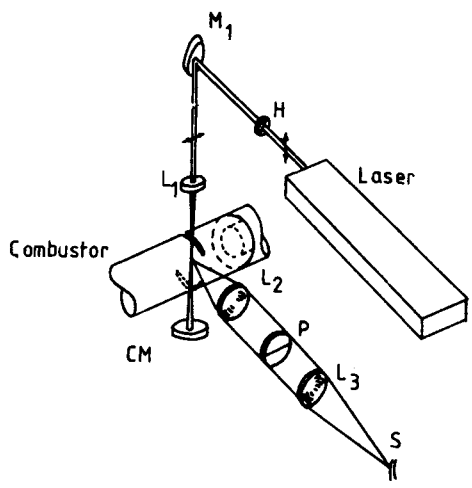

Fig. 2 Schematic of the optical system used for scattering measurements (CM, spherical mirror; H, half-wave plate; M, plane mirror; L, lens; P, polarizer; S, entrance slit of monochromator).

The monochromator is a 1 m Czerny-Turner type and is equipped with a 2000 grove/mm holographic grating for a linear dispersion of 4.8 Å/mm at 2200 Å. Entrance and exit slits are adjusted to give a trapezoidal slit function. The full width at half maximum is 1.3 Å for Raman and 2.7 Å for Rayleigh scattering. Scattered photons are detected by a combination of photomultiplier tube and photon counting electronics with the raw count rate data stored on computer. Photon count rates in the cold reactants are approximately 10^6 Hz for Rayleigh and 2500 Hz for CH_4 Raman. Time-averaged data for both n and CH_4 concentration are obtained with 10 s averaging times, while time-resolved density data are obtained with a 200 μs counting period that gives a frequency response (−3 dB point) of 1.67 kHz.[20]

Finally, the entire optical system including laser and monochromator are mounted on a lathe bed that allows for spatial scanning in a horizontal plane containing the combustor axis. The measurement volume can be located with an accuracy of approximately ±0.5 mm in both the axial and radial directions.

In these experiments, the signal levels are low and the background noise is a problem. Several steps were taken to

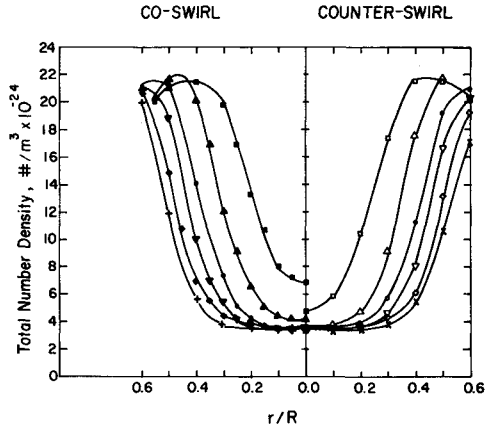

Fig. 3 Radial distributions of time-averaged total number density obtained by Rayleigh scattering for coswirl and counterswirl conditions (■, □ : $X/D = 0.12$; ▲, △ : $X/D = 0.21$; ●, ○ : $X/D = 0.32$; ▼, ▽ : $X/D = 0.38$; ◆, ◇ : $X/D = 0.50$; +, × : $X/D = 0.62$).

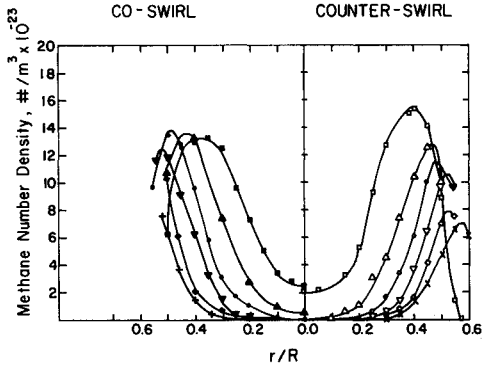

Fig. 4 Radial distributions of time-averaged methane number density obtained by Raman scattering for coswirl and counterswirl conditions (■, □ : $X/D = 0.12$; ▲, △ : $X/D = 0.21$; ●, ○ : $X/D = 0.32$; ▼, ▽ : $X/D = 0.38$; ◆, ◇ : $X/D = 0.50$; +, × : $X/D = 0.62$).

reduce this background to acceptable levels. The test section is a quartz tube of approximately 5 mm wall thickness. Flat black paint was applied to the inner surface of the tube, on the side opposite the collection optics. Pairs of thin slots (1.5 mm wide) were cut in the top and bottom of the tube at six axial positions in the primary region of the combustor to provide entrance and exit points for the laser beam. The edges of these slots and adjoining portions of the tube were also painted black. During the measurements, all but two small segments of the slots, each approximately 1.5 mm long, were closed by taping the exterior of the tube. The flow distortion due to these slots is felt to be small (NB: the wall boundary layer is estimated to be approximately 5 mm thick in this region) and acceptable in view of the problems caused by stray laser light, particularly in the Rayleigh measurements.

Other sources of background noise include thermal emission from the quartz tube and black paint, which is most likely unimportant, and flame radiation. Background measurements with the exciting laser turned off show no significant flame radiation at the Rayleigh (laser) wavelength, but there is a significant background at the Raman wavelength that we conjecture may be due to CO_2 and H_2O emissions. At its peak, this background signal is approximately equal to the total Q-branch signal at high CH_4 densities. Thus, in the Raman measurements, it is necessary to correct for this background and the accuracy of the results is degraded slightly due to shot noise in the background measurement.

The major features of the combustor are described in the introduction; more details can be found in Refs. 5 and 21. The following additional points should be noted. Air is supplied by a blower and at atmospheric pressure without preheat. Mie scattering from dust particles can completely mask Rayleigh scattering from molecules. To control this problem, the flow is filtered twice before entering the combustor. Particle scattering is observed in the data, but the frequency of occurrence is low and no significant error is incurred. The fuel is commercial grade methane supplied in bottles and added to the inner flow at the swirl generator. The air flow is controlled by a combination of gate and butterfly valves and monitored by pressure sensing devices. Swirl levels are determined from inlet velocity profiles obtained in cold flow with a five-hole pressure probe.[21]

Data Analysis

In this paper we report results for the mean total and mean methane number density, rms total number density, and power spectra of total number density. These results are obtained from the photon count data using Eq. (1) after correction is made for background noise and photomultiplier dark count. Appropriate values of K for both Raman and Rayleigh measurements are obtained by calibration in nonreacting flow.

For the Rayleigh measurements, the total background noise contribution (including the dark count) is determined by shifting the collection optics field of view slightly to either side of the scattering volume, as suggested by Lapp et al.[22] While for the Raman measurements, the background is measured directly with the laser turned off.

The raw data from a measurement are of two types: 1) an average, photon count $\bar{N}$ for 10 s and a corresponding estimate of the background for the same period and 2) a set of Rayleigh photon counts $\{N(i,\Delta t)\}$ every 200 μs (Δt) obtained for 5 s. The set $\{N\}$ is made of five independent, continuous time samples each 1 s long, and each N is the sum of counts over a period Δt. Mean values of total number density n and CH_4 concentration are obtained from the type 1 data by subtracting the background counts and dividing by the appropriate product of K, N_0, and the counting period. Shot noise affects these results through both the total photon count measurement and the background count estimate. The resulting uncertainty in the mean densities is less than $\pm 1\%$ in the Rayleigh measurements and from ± 2-9% in the Raman measurements.

From the type 2 data, $\{N(i,\Delta t)\}$, time series data $\{n(i)\}$ for n can be obtained by first subtracting the background count and then dividing by $KN_0\Delta t$. Shot noise in both $\{N\}$ and the background count $\{N_b\}$ contribute to uncertainty levels in the various statistical quantities which are obtained from $\{N(i,\Delta t)\}$.

Correction procedures are available that remove these contributions.[21,23] In the present case, only corrections for shot noise in the signal are necessary and the following equations are used to find the variance, autocorrelation coefficient, and power spectrum:

$$\mathrm{Var}(n) = \overline{n'^2} = [\mathrm{Var}(N) - E(N)]/(KN_0\Delta t)^2 \tag{2}$$

$$R(\tau_r) = (1/\overline{n'^2})[G(\tau_r)/(KN_0\Delta t)^2 - \bar{n}^2] \tag{3}$$

where

$$G(\tau_r) = \sum_i N(i,\Delta t)N(i+\tau_r,\Delta t)$$

$$S(f) = 4\int_0^\infty \overline{n'^2} R(\tau_r)\cos(2\pi f\tau_r)\,\mathrm{d}\tau_r \tag{4}$$

$E(N)$ is the expected value of N.

Results

Measurements are made for one coswirl and one counterswirl flow condition at a total of six axial locations ($x/D = 0.12$, 0.21, 0.31, 0.38, 0.50, and 0.62) in the primary region of the combustor. At each axial location, the measurements are carried out at radial locations on either side of the axis of symmetry. The lateral extent of these measurements is limited by a number of factors: 1) mechanical strength requirements of the quartz test section limit the length of the slots which provide laser light access; 2) fluctuations in Rayleigh scattering cross section increase with increasing radius from approximately $\pm 3\%$ in the undiluted central stream to $\pm 5.5\%$ due to mixing between the two streams; 3) methane is present only in the central stream and in the surrounding annular mixing layer between the two streams.

Operating conditions for the combustor are as follows: $U_i = 31.7$ m/s, $U_o = 22.6$ m/s ($U_i/U_o = 1.4$), $S_i = 0.50$, $S_o = \pm 0.56$, and $\phi_i = 0.80$, where the plus and minus denote coswirl and counterswirl conditions. These conditions are quite similar to those of Refs. 5, 15, and 16. Velocity measurements[15] show that a recirculation zone is present with combustion for both flow conditions.

Time-averaged results are presented first (Figs. 3 and 4). Only radial profiles are presented as the data exhibit good axial symmetry. Since these data are taken over an extended period of time, the repeatability of results is important. In $\bar{n}$ measurements, a repeatability of better than $\pm 4\%$ is achieved, while the corresponding value for Raman scattering is $\pm 6\%$ at high CH_4 concentrations and $\pm 10\%$ at low concentrations.

Both $\bar{n}$ and methane concentration data show a similar reaction zone structure. The data exhibit good axial symmetry. In the mean for both co- and counterswirl, the chemical reaction, as indicated by the presence of large radial gradients in $\bar{n}$ and CH_4 concentration, is confined to a paraboloidal-like sheet that is approximately 2 cm thick with its apex on the centerline near the entrance to the test section. The sheet encloses a region of low-density combustion products with no unreacted fuel. Comparing centerline values for $\bar{n}$ and CH_4, one notes that reaction begins further upstream for the counterswirl condition than for coswirl. Otherwise, the reaction zones for the two flow cases are surprisingly similar in shape.

Dilution of the central fuel/air jet by mixing with the outer flow is evident in both the $\bar{n}$ and CH_4 profiles. With increasing

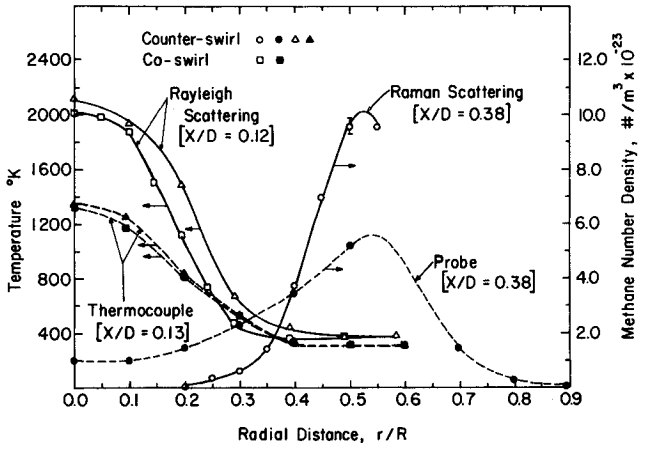

Fig. 5 Comparison of time-averaged methane number density and temperature data obtained by laser scattering measurements with data obtained by probe measurements.

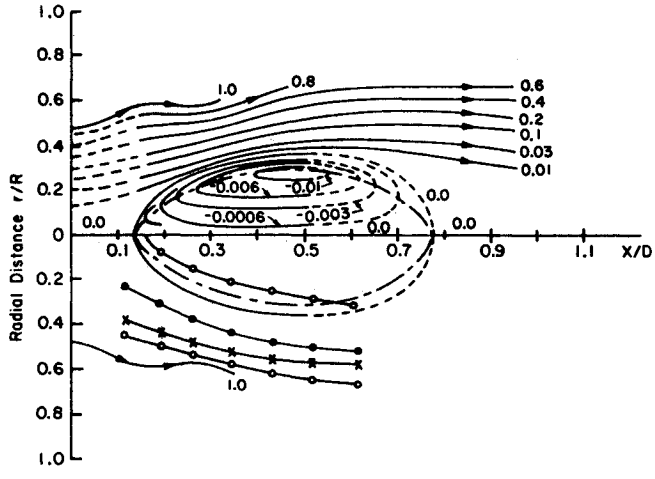

Fig. 6 Flow configuration and density data plot for counterswirl (—streamlines, values normalized by the inner mass flow rate; ---- extrapolations of streamlines; – – – reversed flow zone; • locus of the peak of rms density fluctuation; -o- extent of the reaction zone; -x- locus of the peak of methane concentration).

radius, $\bar{n}$ reaches a maximum and then declines. This decline is attributed to a decrease in σ due to dilution of the central stream with air and, therefore, the observed decline in $\bar{n}$ is spurious. Comparing the coswirl and counterswirl data in Fig. 3, one notes that there is more dilution in counterswirl than in coswirl, which is consistent with the higher turbulence levels observed in the mixing layer between the jets for counterswirl.[15]

The methane data also show that dilution is greater for counterswirl than for coswirl. Two regions of large radial gradients in mean CH_4 concentration are seen on either side of a local maximum value—one due to reaction and the other due to dilution. Note that for both coswirl and counterswirl the CH_4 data indicate the existence of a central core region that is free of dilution and, therefore, in which variations in σ are very small.

A major objective of the methane measurements is to access the accuracy of previously obtained[5] probe data for CH_4 that appeared to be inconsistent with thermocouple results obtained in the same flow. Probe and scattering data for CH_4 are compared in Fig. 5 for $X/D=0.38$; similar results are observed at other axial stations. Considerable discrepancy is present between the two data sets and it must be concluded that the probe results are in error. The cause of this error is unknown. The probe is a cylinder that spans the combustor cross section along a diameter. For such a probe in swirling flow, static pressure gradients drive a secondary flow radially inward in the probe boundary layer, providing one possible explanation for the observed discrepancy. There are other possible explanations. Large probe-induced flow perturbations are frequently reported in the literature for low Reynolds number swirling flows with very thin vortex cores.[3] These perturbations usually involve a displacement of the recirculation zone. In previous studies,[5] it was noted that a flame could be stabilized on the probe if it were placed too close to the test section inlet.

As noted, thermocouple measurements were also performed by Oven et al.[5] The measurement probe consisted of a thermocouple junction held by a cylindrical ceramic support that was inserted into the combustor along a radius. This probe should be less perturbing than the sampling probe and a comparison of thermocouple and scattering data is of interest. To make such a comparison, density data must be converted to temperature data. For an ideal gas, $P=nkT$ and, if pressure is assumed constant, $\bar{T}=(P/k)(\overline{1/n})$. The photon count data $\{N\}$ are converted to $\{n\}$ and $\overline{1/n}$ is calculated without correction for shot noise. Uncertainty in $\bar{T}$ due to shot noise is estimated to be less than 3%. These estimates for $\bar{T}$ are presented along with thermocouple data in Fig. 5.

The two sets of measurements do not compare favorably especially for counterswirl. Note that the data are taken at slightly different axial stations and that the inner flow equivalence ratio is different in the two experiments (0.80 vs 0.78). Due to the difference in mixture ratio, slightly lower values of temperature are expected for the thermocouple data, but 200-800 K differences are not. Lower thermocouple temperatures would also be expected if the probe data are taken further upstream, relative to the reaction zone than the scattering data. However, the probe data are taken at a downstream location. Thus, it appears that the thermocouple probe also gives erroneous results. More research is needed to determine the cause of these observed errors and possible corrections.

Velocity data for this combustor operating under conditions very similar to those of the present study ($\phi_i=0.84$) are available in Ref. 15. Due to seed particle density bias in the LDV data acquisition rate, the measured mean velocities are interpreted as Favre-averaged quantities. With these velocity data and the $\bar{n}$ data, it is possible to estimate the stream function for the two operating conditions studied,

$$\bar{\psi}_r=\int^r 2\pi\left(\frac{W}{A}\right)\bar{n}\tilde{u}r\,dr \tag{5}$$

where the mixture molecular weight W is assumed to be constant. $\bar{\psi}_r$ is determined by numerical integration of Eq. (5) at four axial stations for coswirl ($X/D=0.17$, 0.26, 0.47, and 0.95) and four axial stations for counterswirl ($X/D=0.16$, 0.26, 0.47, and 0.95) where velocity data are available.[15] $\bar{n}$ is obtained at these stations by interpolation of the data shown in Fig. 3. Stream function plots are presented in Figs. 6 and 7 with the values normalized by the inner jet mass flow rate. The dashed lines indicate extrapolated values. In the lower halves of these two figures, the time mean reaction zone and the loci of maximum rms density fluctuation and of maximum CH_4 concentration are indicated. Together this information provides a good picture of the mean flow structure and of the mean reaction zone location.

The recirculation zone is considerably larger in counterswirl than in coswirl; this is true both for length and width as well as for the recirculating mass flow rate. In either case, the total recirculating mass flow rate is a small percentage of the inner flow, approximately 1 and 0.2%, respectively. The reaction zone begins well upstream of the recirculation zone and for the most part lies outside it. In coswirl, there is considerable overlap between the time mean recirculation zone and the reaction zone that seems anomalous, in that near the centerline in the recirculation zone the mean flow is from a region of hot products into the apparent time mean reaction

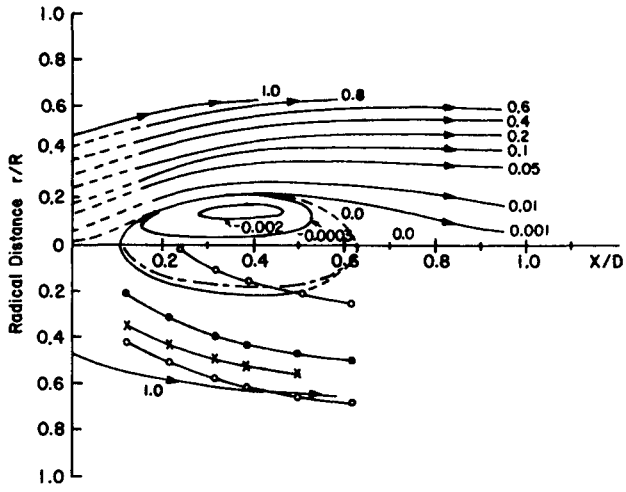

Fig. 7 Flow configuration and density data plot for coswirl (legend same as Fig. 6).

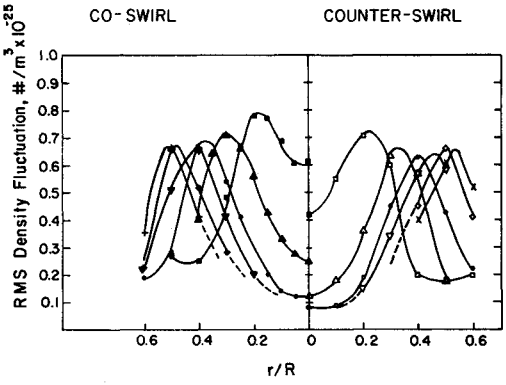

Fig. 8 Radial distributions of rms number density fluctuation data obtained by Rayleigh scattering for coswirl and counterswirl conditions (■, □ :$X/D = 0.12$; ▲, △ :$X/D = 0.21$; ●, ○ :$X/D = 0.31$; ▼, ▽ :$X/D = 0.38$; ◆, ◇ :$X/D = 0.50$; +, × :$X/D = 0.62$).

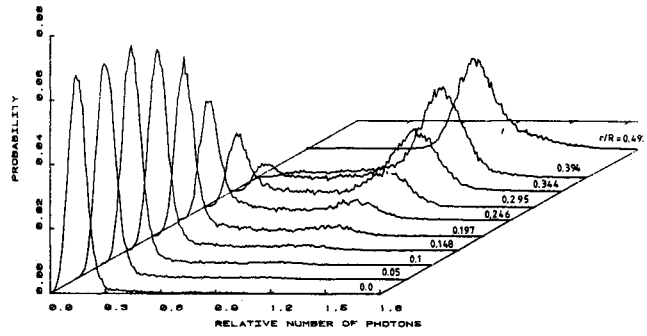

Fig. 9 Typical pdf's of Rayleigh scattered photon arrivals obtained at different radial locations for $X/D = 0.21$ and the coswirl condition. Number of photons is normalized by the value for cold reactants. Note the clear evolution in the pdf's from the reactant to product side as r/R decreases.

zone instead of the reverse, which is the expected behavior. As discussed below, this behavior may be the result of discrete frequency axial oscillations of the recirculation zone. The locus of CH_4 maxima lies on the cold side of the reaction zone, as expected, and inside the $\bar{\psi} = 1.0$ stream surface that marks the center of the mixing layer between the two jets. Note that a significant fraction of the mass flow occurs through an annular region adjacent to the $\bar{\psi} = 1$ stream surface. The effect of the pressure field associated with the recirculation zone and the reaction zone is to push the flow aside, as well as to accelerate it in the axial direction. The axial flow acceleration is quite evident in the velocity data.[15] Finally, we note that the time mean reaction zone seems quite thick relative to the diameter of the recirculation zone and to the thickness of the annular region between the recirculation zone and the interjet mixing layer, a region which the reaction zone fills almost completely.

The time series Rayleigh data are used to find $(\overline{n'^2})^{1/2}$, probability density functions and power spectra for density fluctuations. Some of these results are shown in Figs. 8-11. Because these measurements proved to be extremely time consuming, the measurements were restricted primarily to the reaction zone. So, for instance, there are limited $(\overline{n'^2})^{1/2}$ data available in the recirculation zone. At the different axial measurement stations local maxima in $(\overline{n'^2})^{1/2}$ are observed in the center of the reaction zone and, except for $X/D = 0.12$, these maxima are roughly equal. For small X/D, $(\overline{n'^2})^{1/2}$ is seen to increase in the interjet mixing layer as r/R increases. This change is most likely the result of σ fluctuations due to mixing between the two jet flows. Fluctuation levels in the recirculation zone are for the most part minimal, indicating a region of no significant heat-releasing chemical reactions.

Probability density functions (pdf) constructed from the raw photon count data are bimodal in the reaction zone, which would be expected for a (time mean) reaction zone containing a relatively thin sheet or sheets of chemical reaction separating hot products from cold reactants. Characteristic pdf's are shown in Fig. 9.

Power spectra of the density fluctuations reveal several modes of discrete frequency oscillation in the reaction zone as can be seen in representative spectra, Figs. 10 and 11. Previous velocity and flame emission measurements[9,15,16] indicated the presence of such oscillations, but could not provide much detail concerning frequency and intensity characteristics. Both low (50-100 Hz) and high (400-500 Hz) frequency oscillations are observed with the low-frequency components being more prominent on the centerline than at larger radii. Vu and Gouldin[9] observed high-frequency oscillations that they attributed to instability in the flow entering the test section and described as helical waves rotating at the rotational frequency of the flow. Gouldin et al.[15] suggest that the recirculation zone may undergo axial oscillations of relatively low frequency. We suggest that the oscillations observed here are the result of both phenomena. The low-frequency oscillations are due to recirculation zone movement, while the high-frequency oscillations are helical waves entering the combustor in the inner flow from upstream. These oscillations and our interpretation of them are the subject of another paper.[24]

From Figs. 10 and 11, it is quite clear that the observed oscillations make a significant contribution to $(\overline{n'^2})^{1/2}$ in certain locations. Axial oscillations of the recirculation zone can thicken the mean reaction zone considerably. The observed overlap of the reaction and recirculation zones, which is especially large in coswirl, may be partly or wholly the result of these periodic oscillations. In this regard, we note that the low-frequency oscillations are larger for coswirl than for counterswirl. Oscillations are frequently observed in swirling flows and their role in combustion requires further study.

Discussion

The mean density and concentration data when combined with the velocity data of Ref. 15 provide a good picture of conditions in the primary zone of the combustor. Provided that our interpretation of the effect of recirculation zone oscillations is valid, the reaction zone is seen to lie completely outside the recirculation zone and combustion is stabilized on the centerline in the low-velocity region in front of the oscillating recirculation zone.

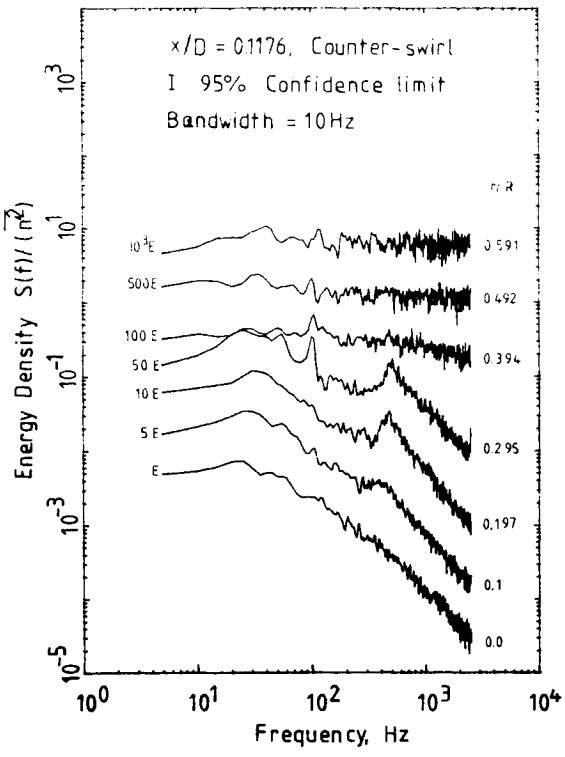

Fig. 10 Typical power spectra of density fluctations obtained for counterswirl condition. For plotting, each curve is scaled by a multiplicative factor the reciprocal of which is shown to the left of its curve. Thus, to obtain the actual energy density, a quantity read from a curve must be multiplied by the appropriate factor on the left.

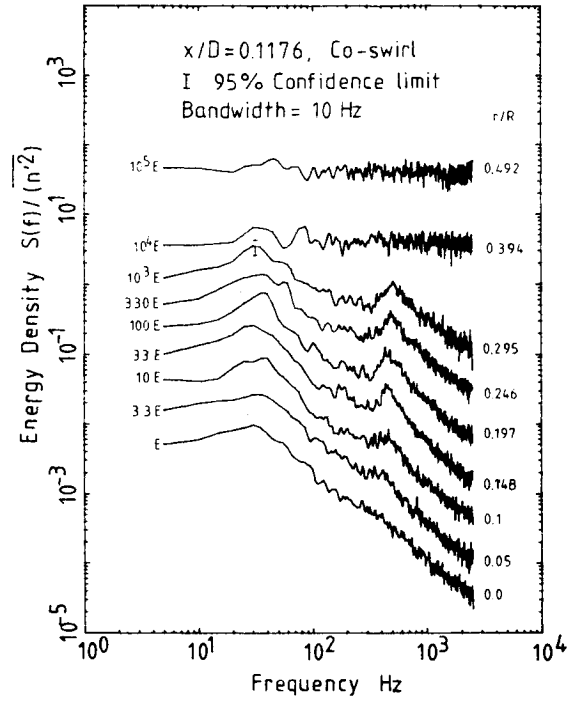

Fig. 11 Typical power spectra of density fluctuations obtained for the coswirl condition. For an explanation of the numerical factors shown to the left of each curve, see the caption of Fig. 10.

Mass flow rates in the recirculation zone are very low and as a consequence we believe that residence times for fluid particles in this zone are long. Also, the recirculation zone is a region of high temperature and, therefore, NO production rates are large. For long residence times, NO concentrations should approach equilibrium values. Thus, NO measurements, free of probe problems, in the recirculation zone should prove quite interesting.

For the time-resolved density measurements, the spatial and temporal resolution are 1 mm and 200 μs, respectively, where 1 mm is the height of the cylindrical scattering volume, while its diameter is 0.1 mm. The adequacy of resolution is difficult to assess. Power spectra data show that fluctuations above 1.67 kHz are low and therefore do not make a significant contribution to $\bar{n}$ and $(\overline{n'^2})^{1/2}$. Furthermore, photon pdf's were calculated at selected points with the data obtained for counting periods of 100, 200, and 500 μs. Little change was seen when comparing pdf's from the 100 and 200 μs data, but at certain locations the 500 μs pdf's were obviously wrong. While shot noise, which varies as $\sqrt{\Delta t}$, introduces some ambiguity into these comparisons, we conclude that our measurements were taken with sufficient temporal resolution to find $\bar{n}$, $(\overline{n'^2})^{1/2}$, and the spectra reported.

During a measurement period Δt, a fluid particle will move a distance $u\Delta t$, where u is the particle speed, and the quantity measured during this period is an average over all the fluid passing through the measurement volume during the period. For $u = 10$ m/s the distance traveled in 200 μs is 2 mm. From this, we conclude that the effective spatial resolution of our measurements is determined by the temporal resolution and that the resolution is satisfactory for our purposes.

Summary

Laser scattering measurements are successful in determining total number density and mean methane concentration in the primary zone of a concentric jet, swirling flow combustor. Measurements are restricted to the central flow region where combustion is stabilized and flow recirculation occurs.

Total number density is determined by Rayleigh scattering with a spatial resolution of 1 mm and a temporal resolution of 200 μs. Because of special circumstances, i.e., the central flow is lean, premixed methane air, scattering cross-section fluctuations are small, and Rayleigh data can be interpreted unambiguously for number density. Stray laser light and Mie scattering from dust particles present problems that require special treatment. Shot noise in the data is significant and its contribution is easily removed during calculations for statistical quantities of interest [see Eqs. (2-4)]. Raman scattering is used to determine mean CH_4 concentration with spatial resolution comparable to that of the Rayleigh measurements. Measurable signal levels are observed from the Raman active ν_1 fundamental oscillation, and good quality time mean data are obtained by long time averaging.

From the mean data a good picture of the primary zone of the combustor is obtained. Reaction occurs in a thick paraboloidal like sheet; its apex anchored on the centerline of the combustor, upstream of the recirculation zone. While the recirculation zone size is quite different for the two flow conditions investigated, the reaction zone shape for the two cases is strikingly similar. Stream surfaces are estimated using the $\bar{n}$ data and previously obtained velocity data. It is seen that much of the inner jet flow is pushed away from both the reaction zone and the recirculation zone as it enters the test section.

Comparison of CH_4 data and temperature data with similar data obtained by probes in a previous study shows significant error in the probe data. Several causes for the observed error are proposed, but more work is required to determine the exact cause and to suggest how these errors might be avoided in the future.

Finally, power spectra of density fluctuations show the presence of discrete frequency oscillations in the combustor. Two types of oscillations are detected: low-frequency oscillations that are attributed to axial oscillations of the recirculation zone and higher-frequency oscillations that are similar to those observed by Vu and Gouldin[9] and on that basis are

assumed to be helical waves triggered by hydrodynamic instability of the inner jet flow before it enters the test section. These fluctuations make a significant contribution to $(\overline{n'^2})^{1/2}$ and may thicken the time mean reaction zone considerably.

Acknowledgment

This work was supported by the U.S. Department of Energy under contract number DE-AC04-77CS04508.

References

[1]Syred, N. and Beer, J. M., "Combustion in Swirling Flow: A Review," *Combustion and Flame*, Vol. 23, 1974, pp. 143-201.

[2]Lilley, D. G., "Swirl Flows in Combustion—A Review," *AIAA Journal*, Vol. 15, 1977, pp. 1063-1078.

[3]Gouldin, F.C., "Probe Measurements in Multi-dimensional Reacting Flows," *Testing and Measurement Techniques in Heat Transfer and Combustion*, AGARD CP-281, 1980, pp. 4-1—4-14.

[4]Gore, R. W. and Ranz, W. E., "Backflows in Rotating Fluids Moving Axially Through Expanding Cross-sections," *AIChE Journal*, Vol. 10, 1964, pp. 83-88.

[5]Oven, M. J., Gouldin, F. C., and McLean, W. J., "Temperature and Species Concentration Measurements in a Swirl Stabilized Combustor," *Seventeenth Symposium (International) on Combustion*, The Combustion Institute, Pittsburgh, PA, 1979, pp. 363-374.

[6]Beltagui, S. A. and MacCallum, N.R.L., "Aerodynamics of Vane-Swirled Flames in Tunnels," *Journal of the Institute of Fuel*, Vol. 49, 1976, pp. 193-200.

[7]Rhode, D. L., Lilley, D. G., and McLaughlin, D. K., "Mean Flowfields in Axisymmetric Combustor Geometries with Swirl," AIAA Paper 82-0177, 1982.

[8]Brum, R. D. and Samuelsen, G. S., "Two Component Laser Anemometry Measurements in a Non-Reacting and Reacting Complex Flow Model Combustor," Paper presented at Fall Meeting of Western States Section of The Combustion Institute, Sandia National Laboratories, Livermore, CA, Rept. WSS/CI 82-53, Oct. 1982.

[9]Vu, B. T. and Gouldin, F. C., "Flow Measurements in a Model Swirl Combustor," *AIAA Journal*, Vol. 20, 1982, pp. 642-651.

[10]Sommer, H. T., "Swirling Flow in a Research Combustor," AIAA Paper 83-0313, 1983.

[11]Martin, D. T., Gouldin, F. C., and Yetter, R. A., "Preliminary Evaluation of a Vortex Breakdown Stabilized Combustor," College of Engineering, Cornell University, Ithaca, NY, Energy Program Rept. EPR-75-9, 1975.

[12]Oven, M. J., McLean, W. J., and Gouldin, F. C., "NO-NO_x Measurements in a Methane Fueled, Swirl-Stabilized Combustor," College of Engineering, Cornell University, Ithaca, NY, Energy Program Dept. EPR-78-5, 1978.

[13]Yetter, R. A. and Gouldin, F. C., "Exhaust Emissions of a Vortex Breakdown Stabilized Combustor," College of Engineering, Cornell University, Ithaca, NY, Energy Program Rept. EPR-77-3, 1977.

[14]Anand, M. S. and Gouldin, F. C., "Combustion Efficiency of a Premixed Continuous Flow Combustor," *Transactions of ASME, Journal of Gas Turbines and Power*, Vol. 107, 1985, pp. 695-705.

[15]Gouldin, F. C., Depsky, J. S., and Lee, S. L., "Velocity Field Characteristics of a Swirling Flow Combustor," *AIAA Journal*, Vol. 23, 1985, pp. 95-102.

[16]Beyler, C. L. and Gouldin, F. C., "Flame Structure in a Swirl Stabilized Combustor Inferred by Radiant Emission Measurements," *18th Symposium (International) on Combustion*, The Combustion Institute, Pittsburgh, PA, 1981, pp. 1011-1019.

[17]Lapp, M. and Penney, C. M., in *Advances in Infrared and Raman Spectroscopy*, Vol. 3, edited by R.J.H. Clark and R. E. Hester, Heyden, London, 1977, Chap. 6.

[18]Setchell, R. E., "Time Averaged Measurements in Turbulent Flows Using Raman Spectroscopy," Sandia Laboratories, Livermore, CA, Energy Rept. SAND 75-8695, 1976.

[19]Dibble, R. W. and Hollenbach, R. E., "Laser Rayleigh Thermometry in Turbulent Flames," *18th Symposium (International) on Combustion*, The Combustion Institute, Pittsburgh, PA, 1981, pp. 1489-1499.

[20]Gouldin, F. C. and Halthore, R. N., "Rayleigh Scattering Measurements in Premixed Flames—One Point, Times Series Date," *Experiments in Fluids*, to appear in 1986.

[21]Halthore, R. N., "Rayleigh and Raman Scattering Measurements for Density in a Swirling Flow Combustor," Ph.D. Thesis, Cornell University, Ithaca, NY, 1984.

[22]Lapp, M., Penney, C. M., and Asher, J. A., "Application of Light Scattering Techniques for Measurements of Density, Temperature and Velocity in Gas Dynamics," Aerospace Research Laboratories, Air Force Systems Command, Rept. ARL 73-0045, April 1973.

[23]Gouldin, F. C. and Dandekar, K. V., "Time Resolved Density Measurements in Premixed Turbulent Flames," *AIAA Journal*, Vol. 22, 1984, pp. 655-663.

[24]Gouldin, F. C., Halthore, R. N., and Vu, B. T., "Periodic Oscillations Observed in Swirling Flows with and without Combustion," *20th Symposium (International) on Combustion*, The Combustion Institute, Pittsburgh, PA, 1985, pp. 269-276.